# Chemical Science

Accepted Manuscript


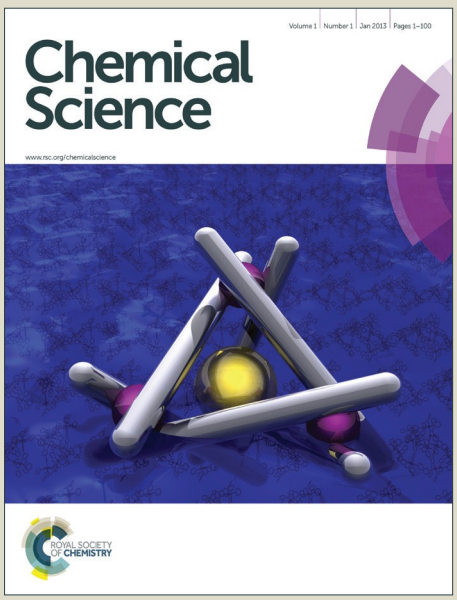





ROYAL SOCIETY OF CHEMISTRY

www.rsc.org/chemicalscience

Journal Name

ARTICLE

# Switching Charge-Transfer Characteristic from *p*-Type to *n*-Type through Molecule "Doping" (Co-crystallization)

Received 00th January 20xx,
Accepted 00th January 20xx

DOI: 10.1039/x0xx00000x

www.rsc.org/

Jing Zhang,[†a] Peiyang Gu,[†a] Guankui Long,[a] Rakesh Ganguly,[b] Yongxin Li,[b] Naoki Aratani,[c] Hiroko Yamada,[c] and Qichun Zhang*[a, b]

Borrowing the idea from silicon industry, where the charge-carrier's characteristic can be changed through heteroatom implantation, we believe that the charge transport nature of organic semiconductors can be switched through molecule "doping" (co-crystallization). Here, we report a novel molecule 2,7-di-tert-butyl-10,14-di(thiophen-2-yl)phenanthro[4,5-abc][1,2,5]thiadiazolo[3,4-i]phenazine (DTPTP), which originally is a p-type (0.3 $cm^2 V^{-1} s^{-1}$) compound, can be switched to a n-type semiconductor ($DTPTP_2$-TCNQ, $3 \times 10^{-3}$ $cm^2 V^{-1} s^{-1}$ in air condition) through tetracyanoquinodimethane (TCNQ) doping (co-crystallization). Single crystal X-ray studies revealed that TCNQ-doped DTPTP complexes ($DTPTP_2$-TCNQ) adopt a dense one-dimensional (1D) mixed π-π stacking mode with the ratio of DTPTP and TCNQ at 2:1 while pure DTPTP molecules utilize a herringbone-packing pattern. Interestingly, theoretical analysis suggests a quasi-2D electron transport network in this host-guest system. Our research result might provide a new strategy to switch charge transport characteristic of one original system by proper molecule "doping" (co-crystal engineering).

## Introduction

Organic semiconductors have attracted widespread interests for their huge applications including radio frequency identification (RFID) tags,[1] electronic papers,[2] optical displays,[3] various sensors,[4a-4d] memory devices[4e-4f] and organic photovoltaics.[5] Comparing with inorganic semiconductors, the structures and properties of organic conjugated materials as well as their solubility and packing in the operation process[6] can be precisely manipulated through organic synthesis. However, a remaining bottleneck faced by organic synthetic chemists is the lack of accurate prediction of the concomitant properties, which resulted in a lot of materials with undesired or even no performance. For example, although huge efforts have been input to prepare organic n-type semiconductors,[7] few of them can meet the basic requirements (e.g. suitable energy level and effective charge transport) for air-stable high performance devices.[8] In addition, introducing too many electron-withdraw elements (e.g. N atom, -F, -CN and so on) into the backbone of the known systems might dramatically change the electron density in π-conjugated frameworks, which makes the targeted compounds extremely unstable. Thus, searching a new method to modify the known systems for the property enhancement or charge-transport switching is highly desirable.[9]

Recently, the construction of multicomponent molecular solids based on molecule "doping" (crystal engineering) has offered a promising alternative way to alter molecular arrangement, change intermolecular interactions, and switch charge transport characteristics, which are totally different from parent single-component materials.[10] For example, 1:1 D-A co-crystals with either mixed stacking or segregated stacking have been prepared by solution process and the as-prepared complexes displayed ambipolar transport properties,[11] light emitting phenomena,[12] photovoltaic effects[13] and so on.[14] The driving forces to form co-crystals during the self-assembly are believed to be *π-π* interaction, charge transfer, or H-bonds.[15] Moreover, the remarkable and promising electronic properties of mixed stacking D-A charge-transfer (CT)-crystals have been theoretically predicted via quantum chemical calculations by Brédas and coworkers,[16] who emphasized the significance of super-exchange along the stacking direction. Zhu et al reported a 1:1 donor–acceptor co-crystal with meso-diphenyl tetrathia[22]annulene[2,1,2,1] (DPTTA) as the donor and extended π-conjugated 4,8-bis(dicyanomethylene)-4,8-dihydrobenzo[1,2-b:4,5-b']-dithiophene (DTTCNQ) as the acceptor, which displayed remarkable high ambipolar transport with both electron and hole mobility exceeding 0.1 $cm^2 V^{-1} s^{-1}$, attributing to the quasi-2D ambipolar transport network.[17] However, other functional complexes with different ratios are rarely reported. One possible reason is that the imbalanced proportion of

[a]*School of Materials Science and Engineering, Nanyang Technological University, Singapore*
E-mail: qczhang@ntu.edu.sg
[b]*Division of Chemistry and Biological Chemistry, School of Physical and Mathematical Sciences, Nanyang Techno logical University, Singapore*
[c]*Graduate School of Materials Science, Nara Institute of Science and Technology, Ikoma, Japan*
† These authors contributed equally to this work.
‡ Electronic Supplementary Information (ESI) available: Additional schemes, figures and tables, characterization of the complexes and pure DTPTP crystal , NMR, HR-MS, TGA, CV, TEM and calculations are included.
See DOI: 10.1039/x0xx00000x

prime components may disturb inherent intermolecular interaction and induce ineffective transport channels. Till now, the research on careful selection of host-guest pair with appropriate frontier molecular orbitals to achieve efficient CT complex system is still in infancy.

Here, we report the synthesis and characterization of a novel organic conjugated molecule 2,7-di-tert-butyl-10,14-di(thiophen-2-yl)phenanthro[4,5-abc][1,2,5]thiadiazolo[3,4-i]phenazine (DTPTP), which originally is a *p*-type compound (0.3 $cm^2 V^{-1} s^{-1}$), can be switched to a *n*-type semiconductor ($DTPTP_2$-TCNQ, mobility: $3 \times 10^{-3}$ $cm^2 V^{-1} s^{-1}$ in air) through tetracyanoquinodimethane (TCNQ) doping (co-crystallization). Comparing with the traditional crystalline complexes, the advantage of this unprecedented sandwich supramolecular system is that both hosts and guests can be assembled into single mixed columns, where small guests are locked by substituted thiophene and butyl groups. Such arrangements can strongly improve the molecule packing density, which will not only enhance good stability of supramolecular framework, but also allow an effective charge transport. So far, this is the first example with different host-guest ratio and optimized highly-ordered packing structure that displays an effective charge transport.

## Results and discussion

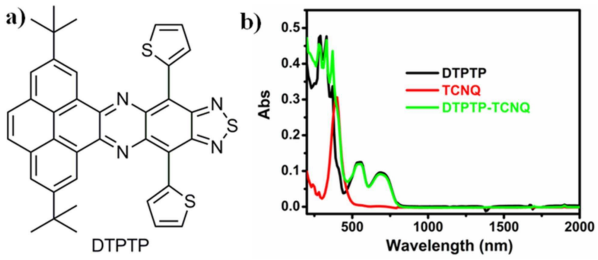


**Fig. 1** (a) Chemical structure of DTPTP; (b) UV-Vis-NIR spectra of DTPTP-TCNQ mixture, DTPTP and TCNQ in toluene.

The synthetic route of the quasi-two dimensional D-A small molecule DTPTP (Fig. 1a) has been provided in supporting information (Scheme S1) and the as-prepared DTPTP has been fully characterized by NMR (Fig. S1), HRMS (Fig. S2), TGA (Fig. S3), and single-crystal XRD. The single crystals of $DTPTP_2$-TCNQ were obtained by slow evaporation of toluene solution containing DTPTP and TCNQ (2:1 ratio).

The UV-vis-NIR absorption spectrum of DTPTP in toluene has been investigated (Fig. 1b). The optical energy bandgap of DTPTP is calculated to be -1.56 eV based on the onset of the absorption spectrum (796 nm) by using the equation of $E_g = 1240/\lambda$. The cyclic voltammetry measurement was performed in a three-electrode system (Figure S4). The LUMO energy level of DTPTP was estimated to be -3.91 eV from the onset reduction potential with reference to $Fc^+/Fc$ (-4.8 eV) using the equation of $E_{LUMO} = -[4.8-E_{Fc} + E_{re}^{onset}]$ eV. The highest occupied molecular orbital (HOMO) energy level of DTPTP is -5.47 eV. These results suggest that DTPTP might have some possible applications in organic electronic devices. Interestingly, the UV-Vis-NIR spectrum (up to 2000nm, Fig. 1b) of the mixed solution (toluene as solvent) containing DTPTP and TCNQ (2:1) almost didn't show any new peaks or peaks shift comparing with that of individual DTPTP or TCNQ in a long wavelength range, which might suggest that no obvious charge-transfer exists in the mixed solution.

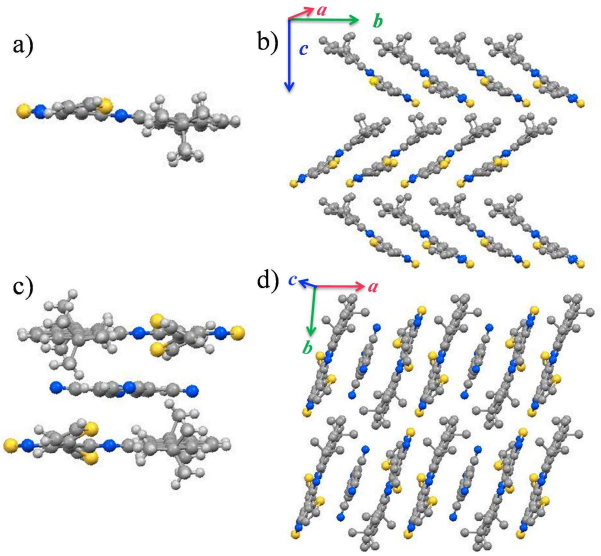


**Fig. 2** Crystal structures of DTPTP and $DTPTP_2$-TCNQ, (a) Molecular structure of DTPTP; (b) Crystal packing of DTPTP (herringbone stacking pattern); (c) Molecular structure of $DTPTP_2$-TCNQ; (d) Crystal packing of the host-guest system (π-π stacking pattern).

The single crystal and packing mode of DTPTP are shown in Fig. 2a and 2b (CCDC number: 1439433). Compound DTPTP crystallized in space group P21/c of the orthorhombic system with unit-cell dimensions of $a$ = 29.6046(8) Å, $b$ = 11.8388(4) Å, $c$ = 17.1781(4) Å, $\alpha$ = 90.00°, $\beta$ = 90.00°, $\gamma$ = 90.00°. The center moiety of DTPTP adopted a slightly twisted structure with a dihedral angle of 5.8°, which was observed between pyrene unit and TQ specie. In this crystal structure, the conformation of substituted individual thiophene groups deviate from main backbone and both of them bent to the second molecule to tighten the stacking. Like the previously reported representative materials (pentacene and rubrene),[18] DTPTP molecules stack into a herringbone arrangement with $\pi$-stacking interactions along the $b$-axis direction, resulting in the efficient electronic couplings and transfer integral along this direction (Fig. 2b). $DTPTP_2$-TCNQ crystallized in space group P-1 (triclinic system, CCDC number: 1439434) with the unit-cell dimensions of $a$ = 10.6919(2) Å, $b$ = 11.6399(2) Å, $c$ = 14.4791(3) Å, $\alpha$ = 90.178(6)°, $\beta$ = 104.400(7)°, $\gamma$ = 95.311(7)°. Fig. 2c shows a component unit of the host-guest co-crystal, where two DTPTP molecules warped above and below the TCNQ molecule, forming a cage to avoid the small additives from escaping. The conformation of the main backbone slightly deviates from the planarity with one thiophene from this molecule bending up and the other one bending down (the bending angle is about 26°). Besides, the large butyl

groups on both sides also lock TCNQ molecules in due to the steric effect. It has been suggested that the degree of charge transfer in a complex can be estimated by the geometry of TCNQ.[19] The ratio $c/(b+d)$ related the length of three bonds in TCNQ (indicated in Fig. S5) was 0.478 for this complex, which is different from the value in neutral TCNQ (0.476). Here, c denotes the length of the isolated carbon-carbon double bond in TCNQ; b and d correspond to the lengths of the carbon-carbon single bonds of the hexatomic ring and outer peripheral, respectively. This result indicates that charge transfer degree between DTPTP and TCNQ is about 0.1. The $\pi$-$\pi$ stacking of sandwich unit forms a linear column structure along the *a*-axis (Fig. 2d). Non-bonded interactions exist between host and guest molecules along these columns. Host-host and host-guest short contacts are also found in neighboring columns (Fig. S6).

Unlike that of other functional complexes (most at 1:1 ratio) reported till now, 2DTPTP and TCNQ molecules stack alternatively into one-dimensional mixed columns along the stacking direction adopting –H–H–G–H–H–G– mode. With the relatively small volume, every two adjacent DTPTP molecules are sandwiched with one TCNQ molecule. The head-to-tail stacking resulted in the efficient overlaps between DTPTP planes, where the terminal pyrene group is considered to have less contribution to $\pi$-conjugated TQ unit. Although there is no expected $\pi$-stacking among guest molecules in the crystal, the direct interactions effect were expected in stacking columns, and lateral interactions in adjacent columns between DTPTP molecules could also be observed, which could serve as the conducting channels.

**Fig. 3** (a, c) Optical micrographs and (b, d) XRD patterns of microcrystals of self-assembled (a, b) DTPTP and (c, d) $DTPTP_2$-TCNQ. In (b) and (d), the peaks are indexed with lattice constants of the bulk crystals.

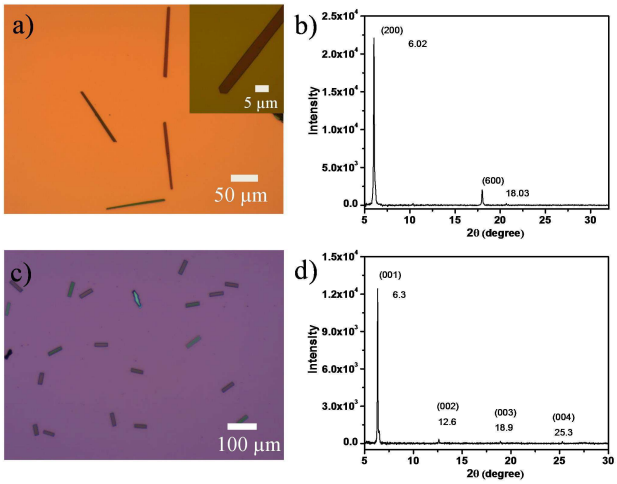


Single-crystalline microribbons/sheets were prepared by drop-casting their toluene solution onto the n-octadecyltrichlorosilane (OTS) modified $SiO_2$ substrates. Optical microscopy (OM) observation revealed that the long DTPTP microribbons exhibit a regular hexagonal shape with tailor angles of 111° as shown in Fig. 3a. The lengths of as-obtained crystalline microribbons are in the range of several tens to hundreds of micrometers. The corresponding X-ray diffraction pattern (Fig. 3b) shows intense peaks at (001), (002) in the crystallographic data of DTPTP. In addition, transmission electron microscopy (TEM) characterization and its corresponding selected area electron diffraction (SAED) (Fig. S7) measurement have been employed to elucidate the structure of DTPTP microribbons. It could be concluded that all single crystals grew along the (010) direction, which is the preferable charge transport direction (*b*-axis). Fig. 3c shows OM picture of $DTPTP_2$-TCNQ parallelogram-like nanosheets, homogeneously covering the substrate with lengths of several tens of micrometers and thicknesses of tens to several hundred nanometers. For the $DTPTP_2$-TCNQ nanosheets, the XRD pattern showed intense peaks at 6.3, 12.6, 18.9, and 20.24°, which were indexed as (001), (002), (003) and (004) in the crystallographic data of $DTPTP_2$-TCNQ, suggesting that the crystals grow with the *ab* plane parallel to the substrate. The growth direction of $DTPTP_2$-TCNQ crystals is determined to be along *a*-axis, the mixed stacking direction (Fig. S8).

**Fig. 4** (a) Transfer and (b) output characteristics of the DTPTP single crystal ribbon device. (c) Transfer and (d) output characteristics of the device based on $DTPTP_2$-TCNQ cocrystal nanosheet.

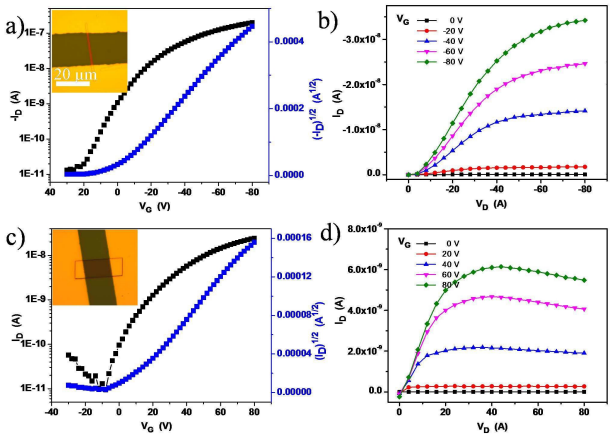


To investigate the influence of TCNQ insertion, we manufactured microcrystal transistor devices (for both DTPTP and $DTPTP_2$-TCNQ) through thermally evaporating Au source/drain electrodes onto the microcrystals via a copper mask to meet the requirements of these single crystals. Copper grid masks were picked up by a tweezer and crossed over the prepared crystals. Subsequently, source/drain electrodes were vacuum-deposited on the structure, and then the "copper grid masks" were peeled off and crystal transistors were fabricated. The typically measured transfer and output characteristics of the devices are shown in Fig. 4. From the transfer characteristics, the devices based on DTPTP single crystals exhibited hole field-effect mobility up to 0.3 $cm^2$ $V^{-1}$ $s^{-1}$ and an on/off ratio of $10^5$ along the *b*-axis under atmospheric conditions (Fig. 4a and b). On the contrary, the devices based on $DTPTP_2$-TCNQ nanosheets displayed typical electron transport properties electron mobility at around 0.003 $cm^2$ $V^{-1}$ $s^{-1}$ and on/off ratio above $10^4$ (Fig. 4c and d). No

*p*-type behavior was observed during the characterization of co-crystal devices and also no *n*-type performance was obtained in DTPTP microcrystal devices. The performances of all the transistors were operated in air, indicating the excellent environmental stability of the *n*-type complex transistors.

To understand the relationship between molecular structure and charge transport properties in the unique $DTPTP_2$-TCNQ host-guest system, the reorganization energies of DTPTP and TCNQ were calculated using a standard four-point method, and the intermolecular electronic couplings between neighbor molecules were obtained through a direct evaluation of the coupling element between frontier orbitals using the unperturbed density matrix of the dimer Fock operator.[20] The electron reorganization energies are 182.5 meV and 253.2 meV for DTPTP and TCNQ, respectively. The intermolecular electronic couplings V ($V_h$ for hole transfer and $V_e$ for electron transfer) for the all fourteen pathways (shown in Fig. S9) are calculated at DFT/PW91PW91/6-31G(d) level, which are given in Table S1. The DTPTP:TCNQ dimer along the $\pi$-$\pi$ stacking (direction 2, as shown in Fig. S9) shows large transfer integral of 19.58 meV for electrons (Fig. 5a,b). To our surprising, the DTPTP:DTPTP dimer in adjacent columns along direction 11 (as shown in Fig. S9) with five-member rings approaching to each other shows even large transfer integral of 25.76 meV for electrons (Fig. 5c,d), which might attribute to the S-S intermolecular interaction, and thus construct a quasi-2D electron transport network. The main electron-transport pathways in the system contain the host-guest pair direction and the host-host pair direction, which indicates that the inserted TCNQ molecules not only transporting electrons but also facilitating the transporting between DTPTP molecules due to the charge-transfer effect and the newly caused packing arrangement. Overall, the transfer integrals for electrons are larger than that of holes, which indicates that DTPTP2-TCNQ facilitates the electron transport other than hole. This is also consistent with our measured results.

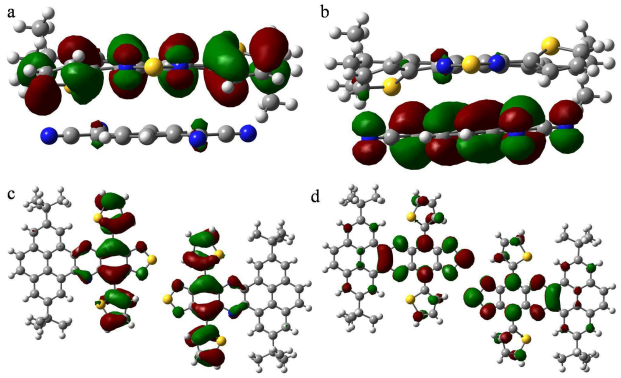


**Fig. 5** The (a) HOMO and (b) LUMO electron density distribution for DTPTP:TCNQ dimer along the $\pi$-$\pi$ stacking direction. The (c) HOMO and (d) LUMO electron density distribution for DTPTP: DTPTP dimer along the direction 11.

## Conclusions

In conclusion, we have demonstrated the charge transport characteristic of DTPTP can be switched from p-type to *n*-type through TCNQ "doping". A 2:1 sandwich-like organic complex ($DTPTP_2$-TCNQ) consisting of a small molecule TCNQ inserting into the center of two interlaced DTPTP planes have been achieved. Intermolecular charge-transfer interaction and terminal groups (thiophene and butyl) cause the self-assembly of stable binary complexes into dense one-dimensional mixed $\pi$-$\pi$ stacking structure. Compared with pure DTPTP which exhibited *p*-type character (0.3 $cm^2\ V^{-1}\ s^{-1}$), the FET devices based on $DTPTP_2$-TCNQ single crystals exhibited *n*-type behavior with electron mobility up to 0.003 $cm^2\ V^{-1}\ s^{-1}$ in ambient atmosphere. Our results might provide a new insight for the design and preparation of intelligent materials for high performance organic electronics and photoelectric devices.

## Experimental

### Materials

Tetrahydrofuran was dried with sodium before using and methylene chloride (DCM) was dried with calcium hydroxide before using. The other chemical reagents and solvents were purchased and used as received without further purification.

### Synthesis

Synthesis of 2,7-di-tert-butyl-10,14-di(thiophen-2-yl)phenanthro[4,5-abc][1,2,5 ]thiadiazolo[3,4-i]phenazine (DTPTP): To a mixture of 4,7-di(thiophen-2-yl)benzo[c][1,2,5]thiadiazole-5,6-diamine (660 mg, 2 mmol) and 2,7-di-tert-butylpyrene-4,5-dione (688 mg, 2 mmol) in acetic acid (100 mL) and chloroform (20 mL) was stirred at 100 $^{o}$C under nitrogen for 24 h. After cooling to room temperature, the mixture was poured into methanol and the crude product was purified by column chromatography over silica gel, eluting with dichloromethane/hexane to give purple crystals compound 2,7-di-tert-butyl-10,14-bisthiophen-2-yl)phenanthro[4,5-abc][1,2,5]thiadiazolo[3,4-i] phenazine (663 mg, 1.04 mmol, 52%).

$^1$H NMR (300 MHz, $CDCl_3$) δ 9.95 (d, *J* = 1.8 Hz, 2H), 9.15 (d, *J* = 3.6 Hz, 2H), 8.30 (d, *J* = 1.7 Hz, 2H), 8.02 (s, 2H), 7.84 (d, *J* = 5.2 Hz, 2H), 7.50 – 7.38 (m, 2H), 1.27 (s, 18H).

HR-MS, calcd for $C_{38}H_{31}N_4S_3$, 639.1711; found, 639.1694.

$^{13}$C NMR could not be obtained due to the solubility of DTPTP.

### Growth of the micro-crystals and device fabrication

The $SiO_2$/Si substrate was heavily doped n-type Si wafer with a 500 nm thick $SiO_2$ layer and a capacitance of 7.5 $nF{\cdot}cm^{-2}$. Bare substrates were successively cleaned with pure water, piranha solution ($H_2SO_4$:$H_2O_2$ = 2:1), pure water and pure isopropanol. Treatment of Si/$SiO_2$ wafer with OTS used in the present study was carried out by vapor deposition method. The clean wafers were dried under vacuum at 90 °C for 0.5 h in order to eliminate the influence of the moisture. After cooling to room temperature, a little drop of OTS was placed on the wafers. Subsequently, this system was heated to 120 °C and maintained for 2 h under vacuum. Micrometer-sized single

crystals of $DTPTP_2$-TCNQ and DTPTP were conducted by using the drop-casting method. After stirring DTPTP and TCNQ (2:1 ratio) in toluene for a long time (about two days), a mixed solution was obtained. A toluene solution containing $DTPTP_2$-TCNQ or DTPTP (~0.5 mg $mL^{-1}$) was poured over the substrates and the solvent evaporated at room temperature. Drain and source Au electrodes (50 nm thickness) were deposited on the crystal by thermal evaporation with a copper grid as the shadow mask.

#### Measurements

HR-MS (ESI) was recorded on a Waters Q-Tof premierTM mass spectrometer. $^1$H NMR spectra were recorded on a Bruker 300-MHz spectrometer. The investigation of UV-vis absorbance was carried out on Shimadzu UV-2501 spectrophotometer. Cyclic voltammetry was carried out with CHI 604E Electrochemical Analyzer. Glassy carbon (diameter: 1.6 mm; area 0.02 $cm^2$) was used as working electrode, platinum wires were used as counter electrode and reference electrode, respectively. Potentials were recorded versus Pt in a solution of anhydrous DCM with 0.1 M tetrabutylammonium hexafluorophosphate ($n$-$Bu_4NPF_6$) as supporting electrolyte at a scan rate of 100 mV $s^{-1}$. $Fc^+$/Fc was used as an internal standard, which has a HOMO energy level of -4.80 eV. Single-crystal diffraction analysis data were collected at 90 K with a BRUKER-APEX II X-ray diffractometer equipped with a large area CCD detector by using graphite monochromated Mo-K$\alpha$ radiation ($\lambda$ = 0.71069 Å). The structures were solved and refined by SHELXL-97 program. The hydrogen atoms were located at geometrically calculated positions and sometimes were not refined. The geometry structures were optimized by using DFT calculations (B3LYP/6-31G*), and the frequency analysis was followed to assure that the optimized structures were stable states. All calculations were carried out using *Gaussian 09.*[21]

#### Quantum simulations

The electronic coupling for the hole and electron can be obtained by using Prof. Shuai's code based on Eq. 1.

$$V = \frac{H_{12} - \frac{1}{2}(H_{11} + H_{22})S_{12}}{1 - S_{12}^2} \quad (1)$$

$H$ is the self-consistent Hamiltonian matrix of the dimer and $S_{12}$ is the overlap integral. The $H$ matrix elements are calculated by $H_{ij} = \langle \phi_i | H | \phi_j \rangle$, where $\varphi_i$ and $\varphi_j$ represent the lowest unoccupied molecular orbitals (LUMOs) for electron transport of isolated molecules in the dimer.

## Acknowledgements

The authors thank Mr. Changli Chen and Prof. Zhigang Shuai from Tsinghua University for their assistance in the transfer integral calculation, Q.Z. acknowledges the financial support AcRF Tier 1 (RG 13/15 and RG 133/14) and Tier 2 (ARC 2/13) from MOE, CREATE program (Nanomaterials for Energy and Water Management) from NRF, Singapore. H.Y. acknowledges the financial support by Grants-in-Aid for Scientific Research (KAKENHI) Nos. 25288092, 26620167 and 26105004 from the Japan Society for the Promotion of Science (JSPS).

## Notes and references

1 G. Gelinck, P. Heremans, K. Nomoto and T. D. Anthopoulos, *Adv. Mater.,* 2010, **22**, 3778.

2 a) G. H. Gelinck, H. E. Huitema, E. van Veenendaal, E. Cantatore, L. Schrijnemakers, J. B. van der Putten, T. C. Geuns, M. Beenhakkers, J. B. Giesbers, B. H. Huisman, E. J. Meijer, E. M. Benito, F. J. Touwslager, A. W. Marsman, B. J. van Rens and D. M. de Leeuw, *Nat. Mater.,* 2004, **3**, 106; b) H. E. A. Huitema, G. H. Gelinck, J. van der Putten, K. E. Kuijk, C. M. Hart, E. Cantatore, P. T. Herwig, A. van Breemen and D. M. de Leeuw, *Nature,* 2001, **414**, 599.

3 a) B. Comiskey, J. D. Albert, H. Yoshizawa and J. Jacobson, *Nature,* 1998, **394**, 253; b) D. Tobjork and R. Osterbacka, *Adv. Mater.,* 2011, **23**, 1935.

4 a) T. Someya, A. Dodabalapur, J. Huang, K. C. See and H. E. Katz, *Adv. Mater.,* 2010, **22**, 3799; b) A. N. Sokolov, M. E. Roberts and Z. A. Bao, *Mater. Today,* 2009, **12**, 12; c) L. Torsi, M. Magliulo, K. Manoli and G. Palazzo, *Chem. Soc. Rev.,* 2013, **42**, 8612; d) J. Li and Q. Zhang, *ACS Appl. Mater. Interfaces*, 2015, **7**, 28049; e) C. Wang, P. Gu, B. Hu, and Q. Zhang, *J. Mater. Chem. C* 2015, **3**, 10055; f) G. Li, K. Zheng, C. Wang, K. S. Leck, F. Hu, X. W. Sun, Q. Zhang, *ACS Appl. Mater. interface* 2013, **5**, 6458; g) B. Hu, C. Wang, J. Wang, J. Gao, K. Wang, J. Wu, G. Zhang, W. Cheng, B. Venkateswarlu, M. Wang, P. S. Lee and Q. Zhang, *Chem. Sci.* 2014, **5**, 3404.

5 a) Y. Lin, Y. Li and X. Zhan, *Chem. Soc. Rev.,* 2012, **41**, 4245; b) W. Cao and J. Xue, *Energy Environ. Sci*., 2014, **7**, 2123; c) A. J. Heeger, *Adv. Mater*., 2014, **26**, 10; d) Q. Zhang, J. Xiao, Z. Y. Yin, H. M. Duong, F. Qiao, F. Boey, X. Hu, H. Zhang, and F. Wudl, *Chem. Asian. J.* 2011, **6**, 856.

6 a) C. Wang, H. Dong, W. Hu, Y. Liu and D. Zhu, *Chem. Rev.,* 2012, **112**, 2208; b) J. Mei, Y. Diao, A. L. Appleton, L. Fang and Z. Bao, *J. Am. Chem. Soc.,* 2013, **135**, 6724.

7 a) Y. Yamaguchi, K. Ogawa, K. Nakayama, Y. Ohba and H. Katagiri, *J. Am. Chem. Soc.,* 2013, **135**, 19095; b) W. Chen, J. Zhang, G. Long, Y. Liu and Q. Zhang, *J. Mater. Chem. C,* 2015, **3**, 8219; c) C. Wang, J. Zhang, G. Long, N. Aratani, H. Yamada, Y. Zhao and Q. Zhang, *Angew. Chem. Int. Ed.* 2015, **54**, 6292. d) Y. Zhao, Y. Guo and Y. Liu, *Adv. Mater.,* 2013, **25**, 5372.

8 a) A. Lv, S. R. Puniredd, J. Zhang, Z. Li, H. Zhu, W. Jiang, H. Dong, Y. He, L. Jiang, Y. Li, W. Pisula, Q. Meng, W. Hu and Z. Wang, *Adv. Mater.,* 2012, **24**, 2626; b) T. He, M. Stolte and F. Wurthner, *Adv. Mater.,* 2013, **25**, 6951; c) F. Zhang, Y. Hu, T. Schuettfort, C. A. Di, X. Gao, C. R. McNeill, L. Thomsen, S. C. Mannsfeld, W. Yuan, H. Sirringhaus and D. Zhu, *J. Am. Chem. Soc.,* 2013, **135**, 2338; d) W. Chen, J. Zhang, G. Long, Y. Liu, and Q. Zhang, *J. Mater. Chem. C* 2015, **3**, 8219.

9 a) B. D. Naab, S. Himmelberger, Y. Diao, K. Vandewal, P. Wei, B. Lussem, A. Salleoa and Z. Bao, *Adv. Mater.,* 2013, **25**, 4663; b) J. Zhang, G. Zhao, Y. Qin, J. Tan, H. Geng, W. Xu, W. Hu, Z. Shuai and D. Zhu, *J. Mater. Chem. C,* 2014, **2**, 8886.

10 a) H. Mendez, G. Heimel, S. Winkler, J. Frisch, A. Opitz, K. Sauer, B. Wegner, M. Oehzelt, C. Rothel, S. Duhm, D. Tobbens, N. Koch and I. Salzmann, *Nat. Commun.,* 2015, **6**. doi:10.1038/ncomms9560; b) S. Horiuchi, K. Kobayashi, R. Kumai, N. Minami, F. Kagawa and Y. Tokura, *Nat. Commun.,* 2015, **6**. doi:10.1038/ncomms8469; c) K. P. Goetz, D. Vermeulen, M. E. Payne, C. Kloc, L. E. McNeil and O. D. Jurchescu, *J. Mater. Chem. C,* 2014, **2**, 3065.

11 a) J. Zhang, H. Geng, T. S. Virk, Y. Zhao, J. Tan, C.-A. Di, W. Xu, K. Singh, W. Hu, Z. Shuai, Y. Liu and D. Zhu, *Adv. Mater.,* 2012, **24**, 2603; b) S. K. Park, S. Varghese, J. H. Kim, S. J. Yoon, O. K. Kwon, B. K. An, J. Gierschner and S. Y. Park, *J. Am. Chem. Soc.,* 2013, **135**, 4757; c) J. Zhang, J. Tan, Z. Ma, W. Xu, G. Zhao, H. Geng, C. a. Di, W. Hu, Z. Shuai, K. Singh and D. Zhu, *J. Am. Chem. Soc.,* 2013, **135**, 558.
12 a) Y. L. Lei, Y. Jin, D. Y. Zhou, W. Gu, X. B. Shi, L. S. Liao and S. T. Lee, *Adv. Mater.,* 2012, **24**, 5345; b) Y. L. Lei, L. S. Liao and S. T. Lee, *J. Am. Chem. Soc.,* 2013, **135**, 3744.
13 a) S. J. Kang, S. Ahn, J. B. Kim, C. Schenck, A. M. Hiszpanski, S. Oh, T. Schiros, Y.-L. Loo and C. Nuckolls, *J. Am. Chem. Soc.,* 2013, **135**, 2207; b) S. J. Kang, J. B. Kim, C.-Y. Chiu, S. Ahn, T. Schiros, S. S. Lee, K. G. Yager, M. F. Toney, Y.-L. Loo and C. Nuckolls, *Angew. Chem. Int. Ed.,* 2012, **51**, 8594.
14 a) A. S. Tayi, A. K. Shveyd, A. C. Sue, J. M. Szarko, B. S. Rolczynski, D. Cao, T. J. Kennedy, A. A. Sarjeant, C. L. Stern, W. F. Paxton, W. Wu, S. K. Dey, A. C. Fahrenbach, J. R. Guest, H. Mohseni, L. X. Chen, K. L. Wang, J. F. Stoddart and S. I. Stupp, *Nature,* 2012, **488**, 485; b) W. Yu, X. Y. Wang, J. Li, Z. T. Li, Y. K. Yan, W. Wang and J. Pei, *Chem. Comm.,* 2013, **49**, 54. c) W. Zhu, R. Zheng, Y. Zhen, Z. Yu, H. Dong, H. Fu, Q. Shi and W. Hu, *J. Am. Chem. Soc.,* 2015, **137**, 11038.
15 a) A. Das and S. Ghosh, *Angew. Chem. Int. Ed.,* 2014, **53**, 2038; b) H. T. Black and D. F. Perepichka, *Angew. Chem. Int. Ed.,* 2014, **53**, 2138.
16 L. Zhu, Y. Yi, Y. Li, E.-G. Kim, V. Coropceanu and J.-L. Brédas, *J. Am. Chem. Soc.,* 2012, **134**, 2340.
17 Y. Qin, J. Zhang, X. Zheng, H. Geng, G. Zhao, W. Xu, W. Hu, Z. Shuai and D. Zhu, *Adv. Mater.,* 2014, **26**, 4093.
18 a) C. Reese and Z. Bao, Mater. Today, 2007, **10**, 20; b) D. Nabok, P. Puschnig, C. Ambrosch-Draxl, O. Werzer, R. Resel and D.-M. Smilgies, *Phys. Rev. B,* 2007, **76**, 235322.
19 T. J. Kistenmacher, T. J. Emge, A. N. Bloch and D. O. Cowan, *Acta Crystallogr. B,* 1982, **38**, 1193.
20 a) E. F. Valeev, V. Coropceanu, D. A. da Silva Filho, S. Salman and J.-L. Brédas, *J. Am. Chem. Soc.,* 2006, **128**, 9882; b) A. Troisi and G. Orlandi, *J. Phys. Chem. B,* 2002, **106**, 2093.
21 (1) Gaussian 09, Revision A.1, M. J. Frisch, G. W. Trucks, H. B. Schlegel, G. E. Scuseria, M. A. Robb, J. R. Cheeseman, G. Scalmani, V. Barone, B. Mennucci, G. A. Petersson, H. Nakatsuji, M. Caricato, X. Li, H. P. Hratchian, A. F. Izmaylov, J. Bloino, G. Zheng, J. L. Sonnenberg, M. Hada, M. Ehara, K. Toyota, R. Fukuda, J. Hasegawa, M. Ishida, T. Nakajima, Y. Honda, O. Kitao, H. Nakai, T. Vreven, J. A. Montgomery, Jr., J. E. Peralta, F. Ogliaro, M. Bearpark, J. J. Heyd, E. Brothers, K. N. Kudin, V. N. Staroverov, T. Keith, R. Kobayashi, J. Normand, K. Raghavachari, A. Rendell, J. C. Burant, S. S. Iyengar, J. Tomasi, M. Cossi, N. Rega, J. M. Millam, M. Klene, J. E. Knox, J. B. Cross, V. Bakken, C. Adamo, J. Jaramillo, R. Gomperts, R. E. Stratmann, O. Yazyev, A. J. Austin, R. Cammi, C. Pomelli, J. W. Ochterski, R. L. Martin, K. Morokuma, V. G. Zakrzewski, G. A. Voth, P. Salvador, J. J. Dannenberg, S. Dapprich, A. D. Daniels, O. Farkas, J. B. Foresman, J. V. Ortiz, J. Cioslowski, and D. J. Fox, Gaussian, Inc., Wallingford CT, 2009.